

Bryan J. Putnam<sup>\*1,2,3</sup>, Ming Xue<sup>1,3</sup>, Guifu Zhang<sup>2,3</sup>, Youngsun Jung<sup>1</sup>, and Nathan Snook<sup>1,3</sup>

Center for Analysis and Prediction of Storms<sup>1</sup>, Atmospheric Radar Research Center<sup>2</sup>, and School of Meteorology<sup>3</sup>, University of Oklahoma, Norman, OK

## Introduction

An important piece of the puzzle for improving numerical weather prediction (NWP) microphysics is improving the representation of the particle size distributions (PSDs) of the hydrometeors used for the initial condition in a forecast, especially for short term convective scale forecasts. Weather radar provides the best temporal and spatial observations of hydrometeors for model initialization. Basically, two approaches currently exist for estimating PSDs from radar data: i) direct observation-based retrieval, and ii) NWP model-based retrieval (i.e., data assimilation (DA)). In direct retrieval, the PSD parameters are estimated from radar reflectivity and/or differential reflectivity. This method normally pre-assumes hydrometeor type and needs at least the same number of independent radar measurements as the number of PSD parameters sought. In reality, however, multiple species of hydrometeors exist in a convective system and there are more parameters desired than available independent measurements, specifically for multi-moment microphysics schemes in NWP models. In this case, model-based retrieval using the Ensemble Kalman Filter (EnKF) yields promising results. The EnKF uses ensemble covariances to update the microphysical state variables based on both observed reflectivity ( $Z$ ) and radial velocity ( $V_r$ ). These state variables can then be used to prognose the DSD parameters.

For this study, the EnKF was applied to a mesoscale convective system (MCS) that passed over western Oklahoma early on May 9 2007. Both a single-moment (SM) Lin three-ice microphysics scheme and a Milbrandt and Yau double-moment (DM) scheme were used in multiple experiments. Previous research has shown that use of a DM scheme over a SM scheme results in a significant improvement in the representation of the microphysical state of supercells, specifically the size sorting of hydrometeors. The event was observed by KOUN, a dual-polarimetric WSR-88D radar. The polarimetric radar measurements provide additional information on the PSDs of the hydrometeors present than reflectivity ( $Z$ ) alone, such as the size of rain drops and the presence of hail. A polarimetric radar simulator (Jung et al. 2008a, 2010) that calculates several variables including differential reflectivity ( $Z_{dr}$ ), specific differential phase ( $K_{dp}$ ), and cross-correlation coefficient ( $\rho_{hv}$ ) using the model state variables was used in conjunction with the polarimetric observations to better assess the microphysical state.

## Methodology

- CAPS Advanced Regional Prediction System (ARPS) fully compressible, non-hydrostatic storm-scale model used.
- Model domain: 259 x 259 x 43 with 2km horizontal resolution and stretched vertical resolution with average distance of 500m
- Initial model variables, lateral boundary conditions, and surface conditions interpolated from 12km NCEP 9 May 2007 0000 UTC NAM model analysis
- One hour deterministic forecast from 0000 UTC to 0100 UTC to "spin-up" the system
- 40 member ensemble generated from 1 hour forecast by adding random, smoothed, Gaussian perturbations to  $u, v, w$ , and  $q$  for all hydrometeors
- Level II  $Z$  and  $V_r$  observations assimilated from 5 regional WSR-88D radars as well as the 4 radars in the CASA network.
- Analysis period consisted of 5 minute forecasts and assimilation cycles ( $Z$  and  $V_r$ ) over a 1 hour period between 0100 and 0200 UTC
- 3 hour deterministic forecast made from the final ensemble mean analysis.
- Microphysics schemes used include mixed SM microphysics between members that consisted of 16 Lin et al. (1983) (LIN) members, 16 Weather research and Forecast (WRF) model SM 6-class microphysics scheme (Hong and Lim 2006) (WSM6) members, and 8 simplified NWP explicit microphysics (NEM) members (Schultz 1995) to increase ensemble spread (Snook et al. 2011) for SM assimilation, and Milbrandt and Yau (MY) (2005) DM microphysics scheme for DM assimilation
- Lin scheme used for SM forecast and MY scheme for DM forecasts
- Intercept parameter used for rain adjusted by a factor of 10 from  $8 \times 10^6 \text{ m}^{-4}$  as is typically used in the LIN scheme to  $8 \times 10^5 \text{ m}^{-4}$
- The shape parameter was set to 0 in all cases

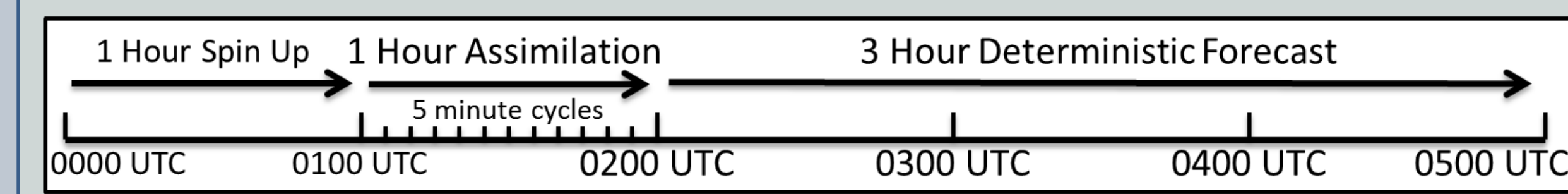


Fig. 1. Diagram of experiment timeline for all experiments listed.

Experiment	Assimilation Scheme	Forecast Scheme	Multi	Noise	Relax	Graupel	Hail
SS_M	SM LIN,WSM6,NEM	SM LIN	0.25	0	0	N	Y
SD_M	SM LIN,WSM6,NEM	DM MY	0.25	0	0	N	Y
DD_M	DM MY	DM MY	0.25	0	0	N	Y
DD_MA	DM MY	DM MY	0.25	$u, v, \theta + .5$	0	N	Y
DD_R	DM MY	DM MY	0.00	0	0.5	N	Y

Table 1. Description of experiments performed including the microphysics scheme used during assimilation and forecast; whether multiplicative inflation, additive noise, or covariance relaxation was used and by what amount; and whether graupel or hail was included. The experiment naming format gives the scheme used for assimilation and forecast followed by the model error treatments used.

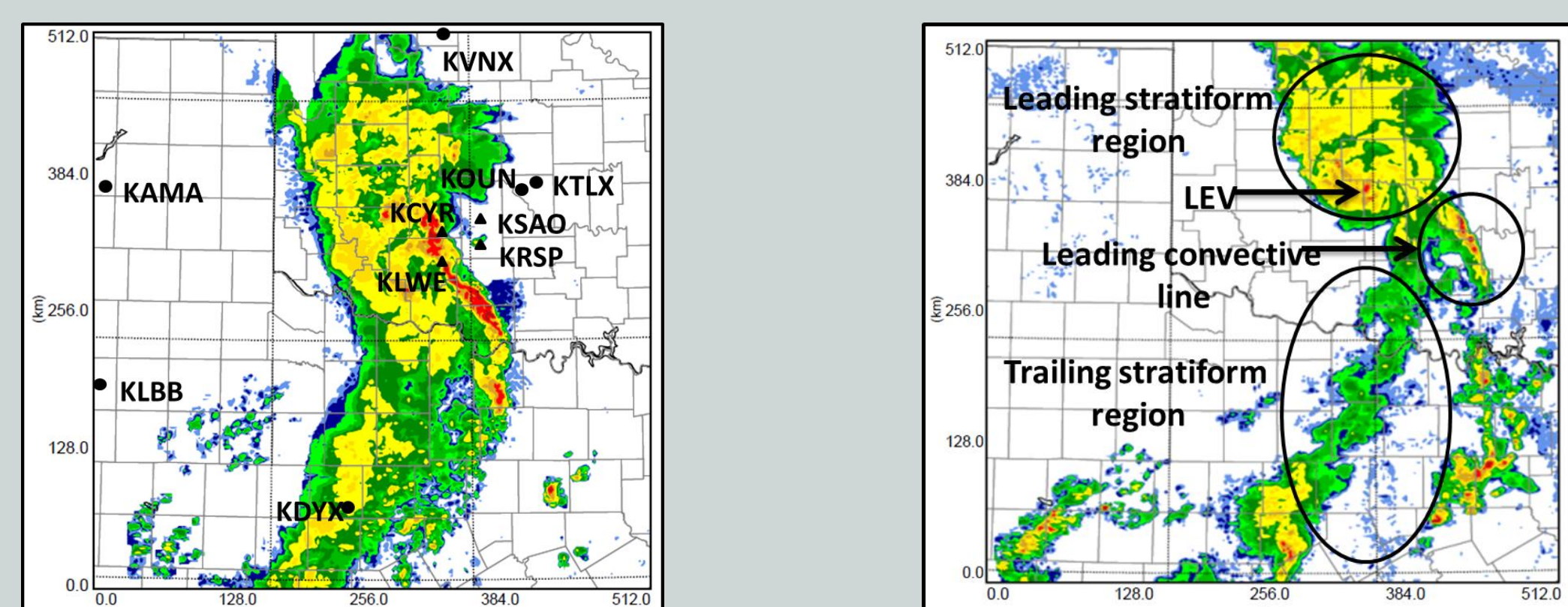


Fig. 2. Locations of radars used for assimilation as well as KOUN used for comparison relative to the MCS at time of final assimilation (0200 UTC) and location of main system features at 0400 UTC.

## Results

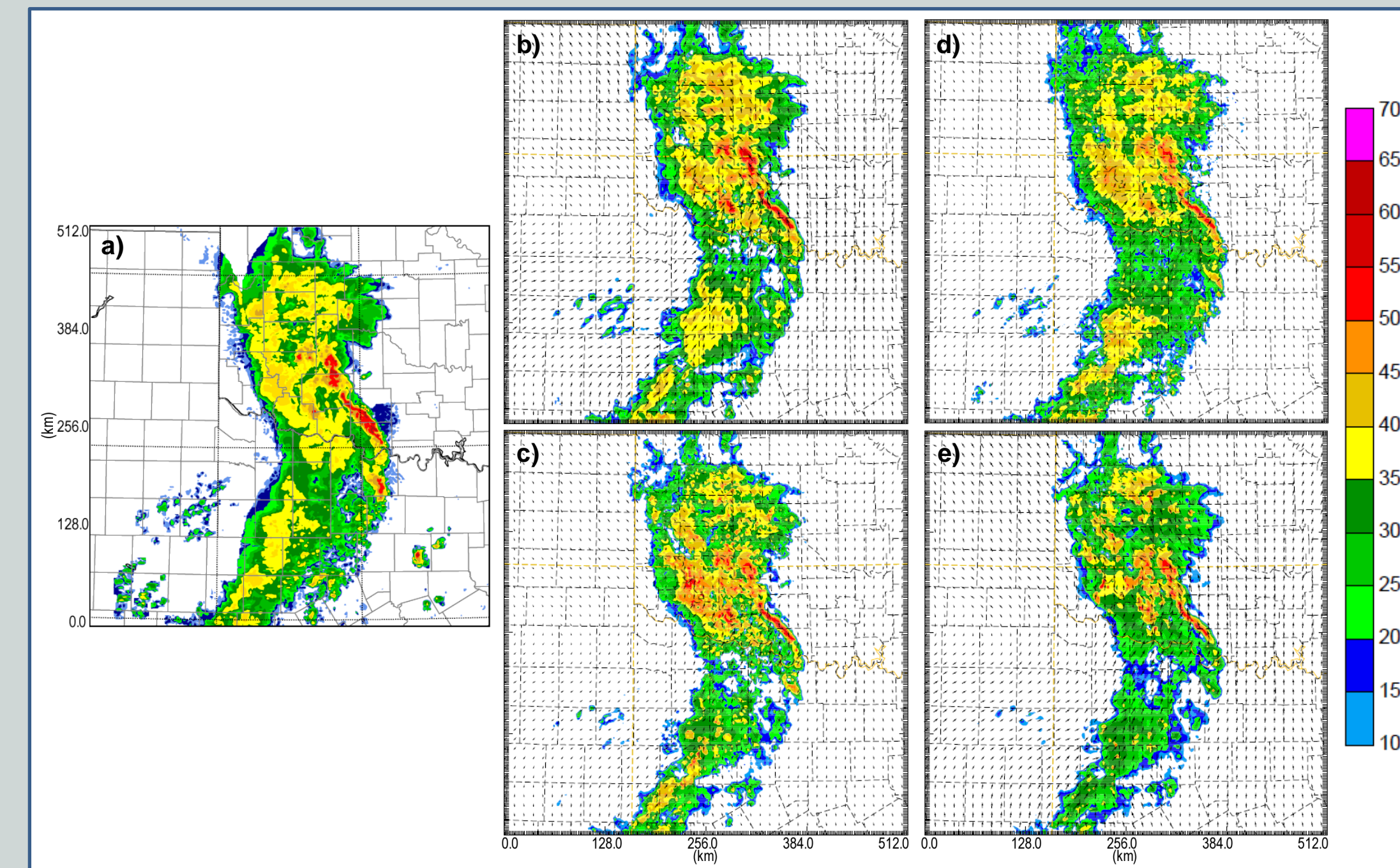


Fig. 3. (a) Observed  $Z$  (dBZ) mosaic as well as final ensemble mean analysis  $Z$  (0200 UTC) from (b) SS\_M, (c) DD\_M, (d) DD\_MA, (e) DD\_R.

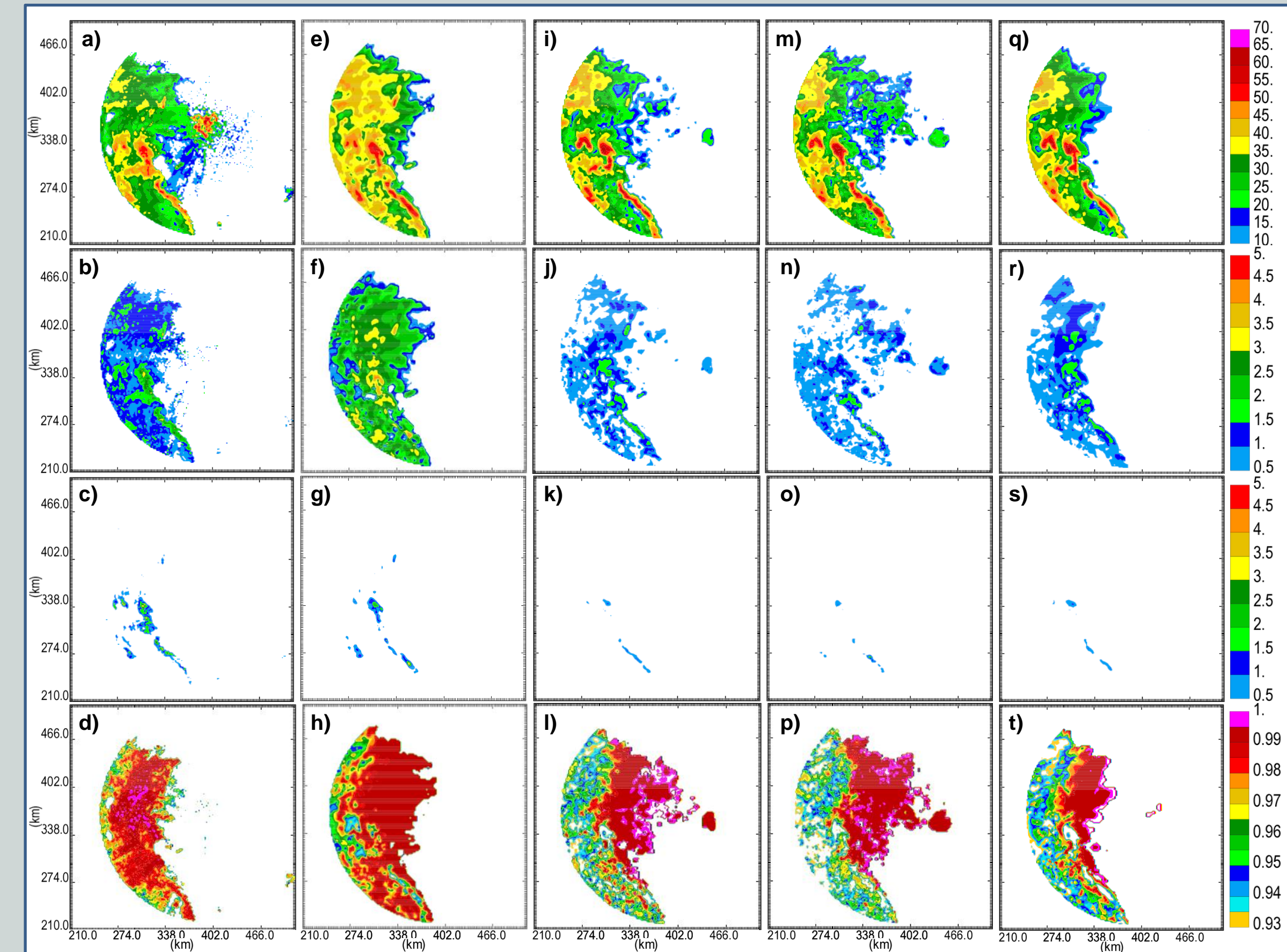


Fig. 4. Observed (a)  $Z$  (dBZ), (b)  $Z_{dr}$  (dB), (c)  $K_{dp}$  (dB km<sup>-1</sup>), and (d)  $\rho_{hv}$  from KOUN at 5' tilt as well as simulated variables for (e-h) SS\_M, (i-l) DD\_M, (m-p) DD\_MA, and (q-t) DD\_R from their respective final ensemble mean analyses at 0200 UTC. Note that the simulated variables are as if they were observed from KOUN.  $Z_{dr}$  results show the size of raindrops in the experiments with the DM scheme match the observations better.

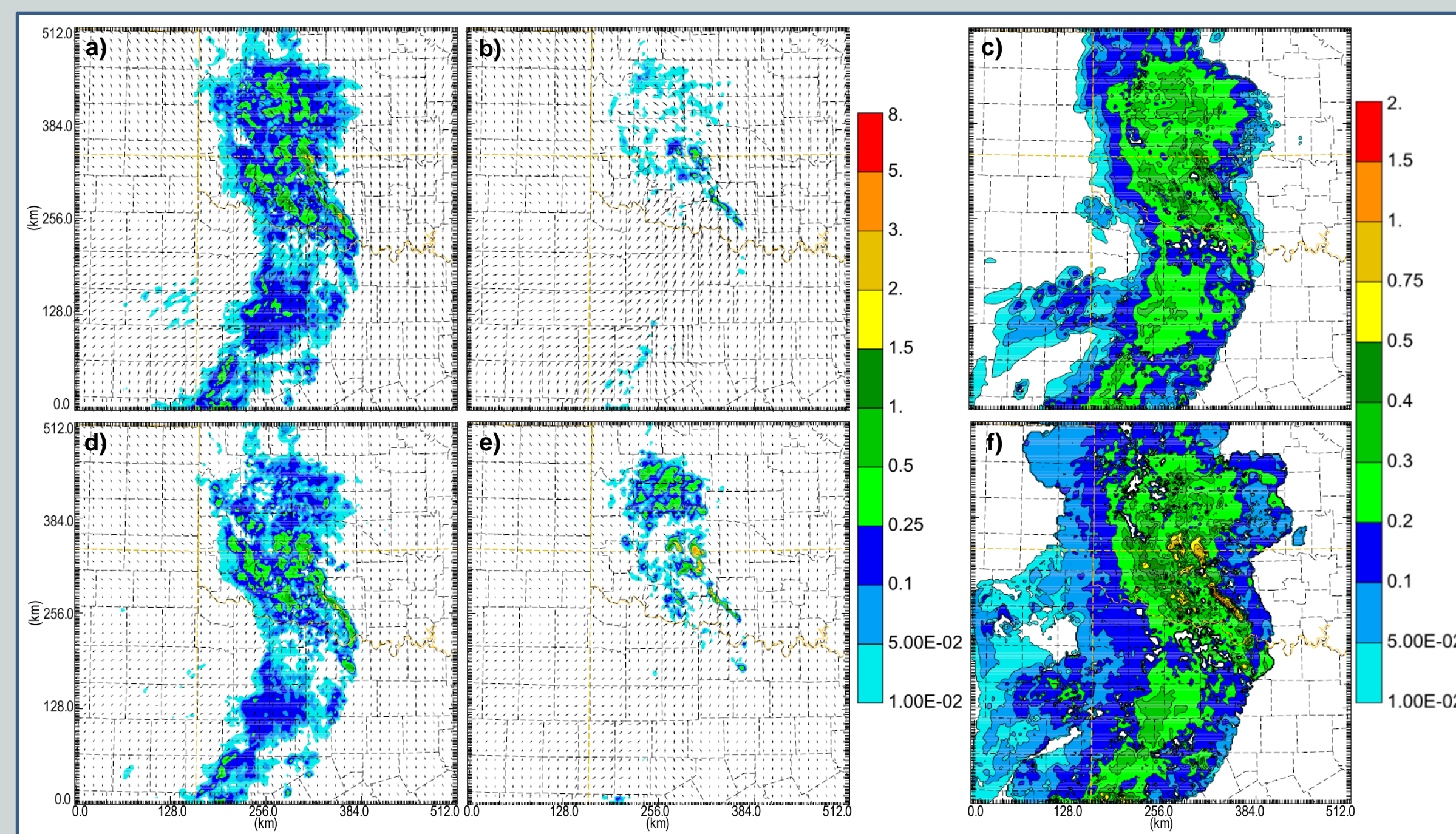


Fig. 5. Final ensemble mean analysis (0200 UTC) (a) rain and (b) hail mixing ratios ( $\text{g kg}^{-1}$ ) and (c) mass weighted median diameter (mm) for SS\_M as well as (d-f) DD\_M. While there is a slightly larger amount of hail in DD\_M, the expected difference in drop sizes between convective and stratiform precipitation is much better represented compared to SS\_M.

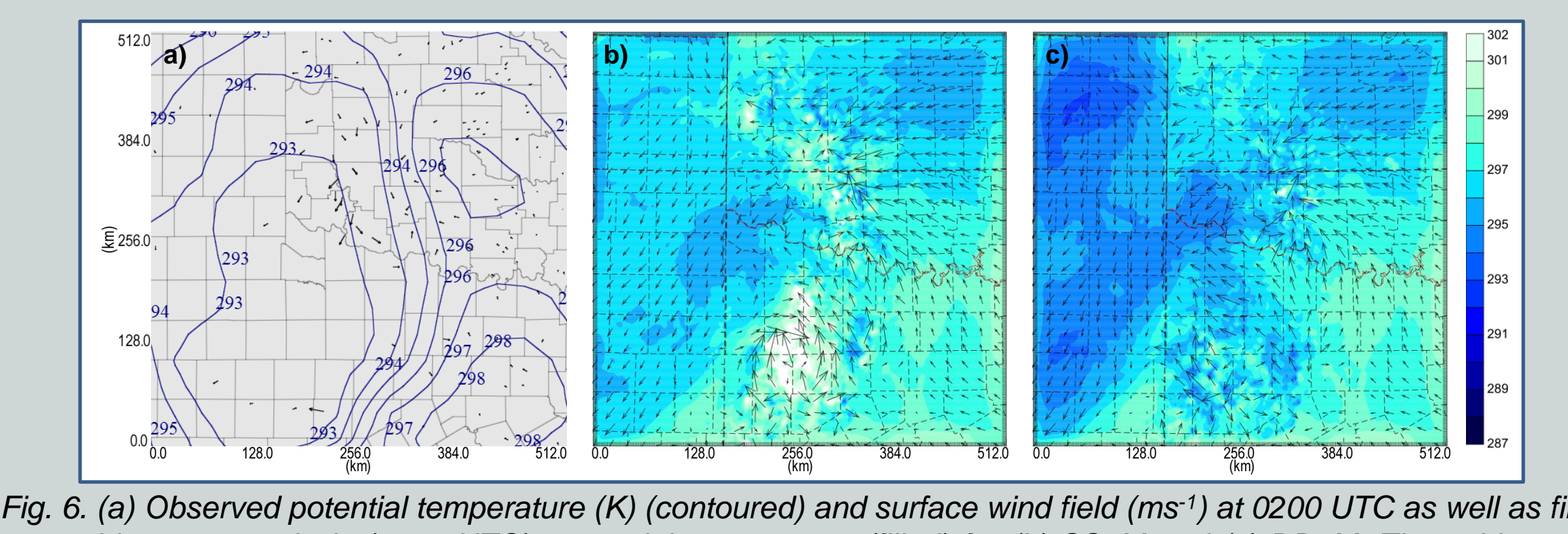


Fig. 6. (a) Observed potential temperature (K) (contoured) and surface wind field ( $\text{ms}^{-1}$ ) at 0200 UTC as well as final ensemble mean analysis (0200 UTC) potential temperature (filled) for (b) SS\_M and (c) DD\_M. The cold pool in DD\_M matches the observations better, is more uniform, and may have led to better preservation of the stratiform region early in the forecast.

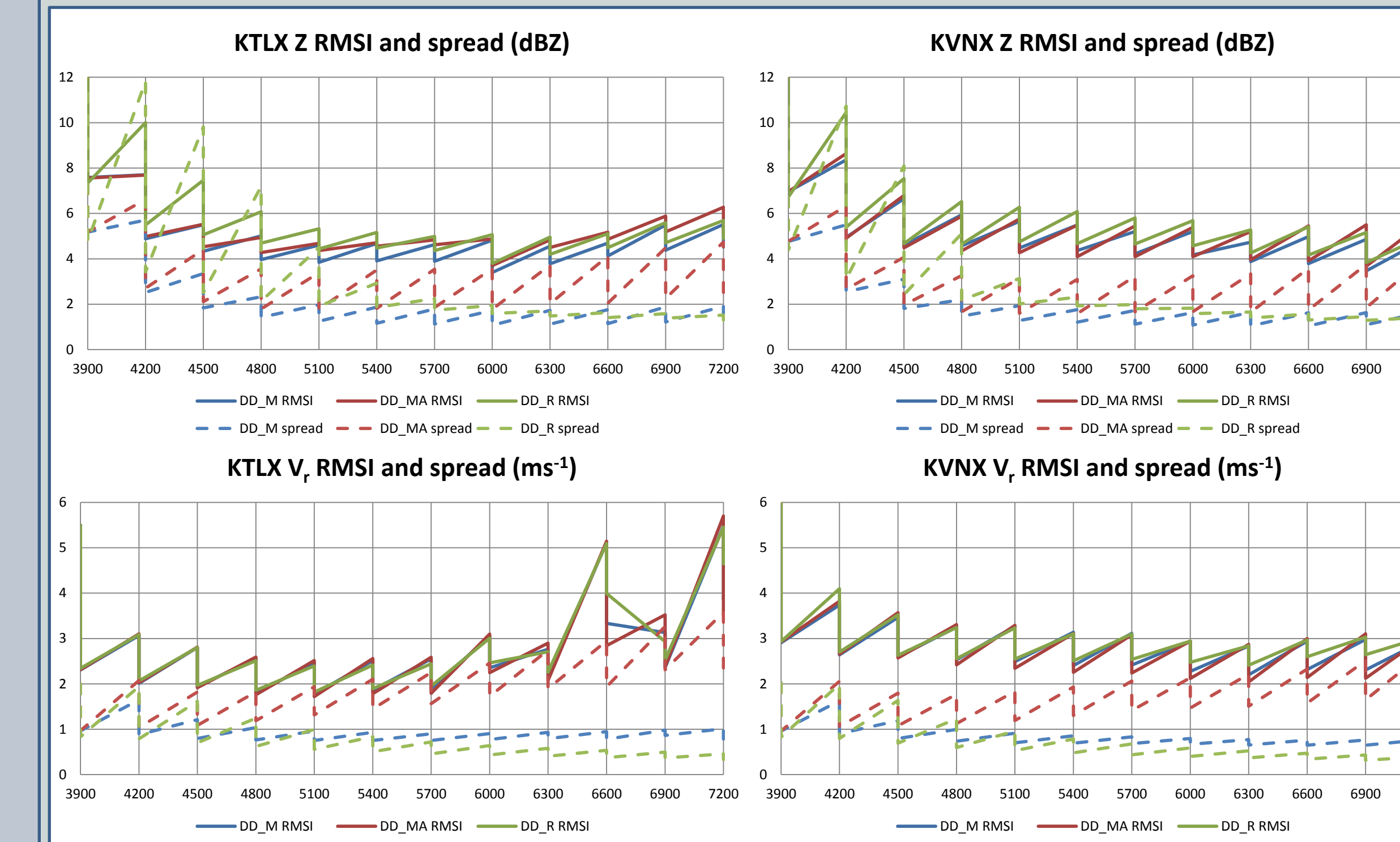


Fig. 7. Root mean square innovation and ensemble spread during assimilation. Note that while additive noise and relaxation increased ensemble spread, neither provided improved RMSI.

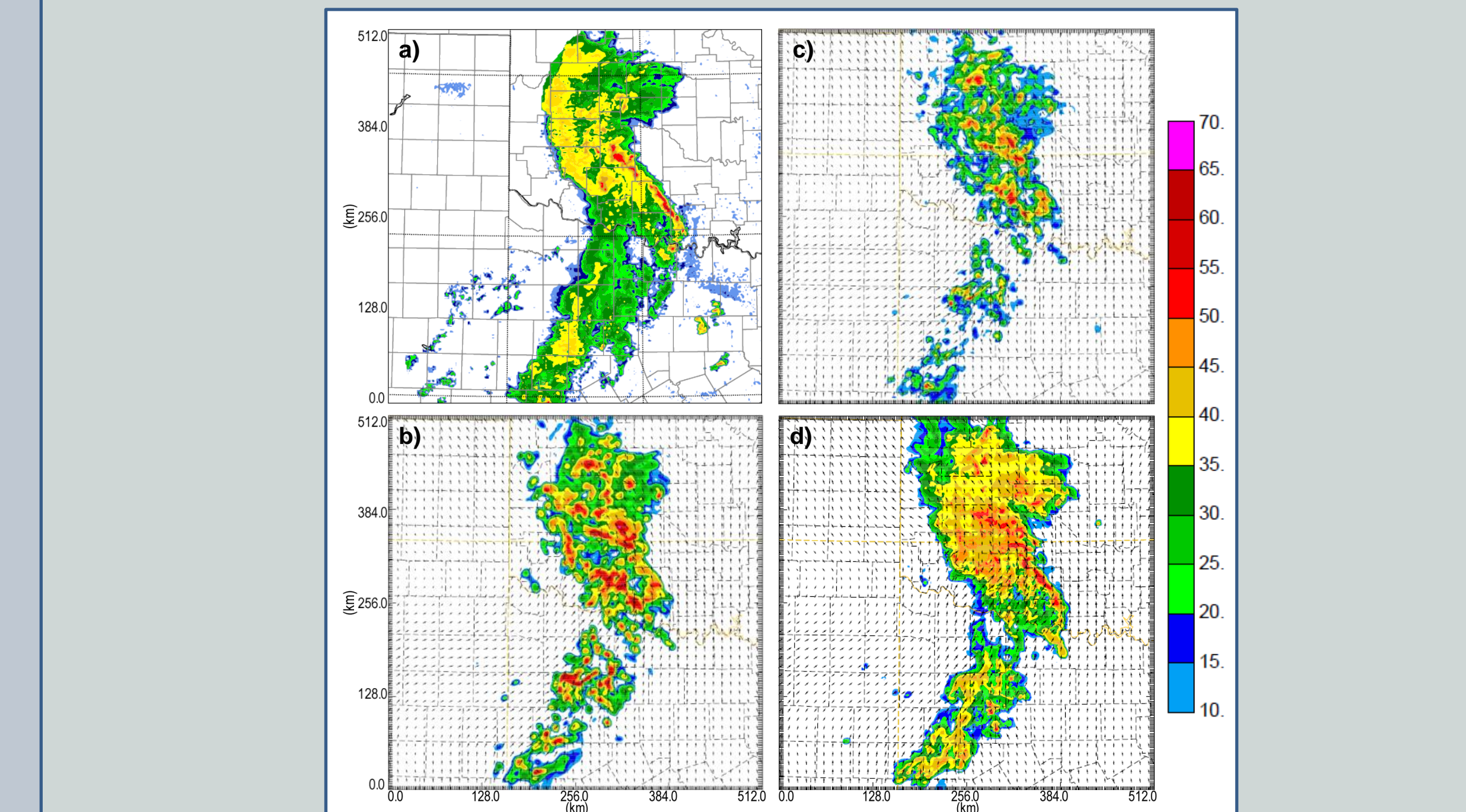


Fig. 8. (a) Observed  $Z$  (dBZ) mosaic at (0230 UTC) as well as 30 minute forecast  $Z$  (020 UTC) from (b) SS\_M (c) SD\_M, and (d) DD\_M. Both results initialized from the SM final analysis broke down into multiple convective cells instead of maintaining a leading convective line and stratiform regions like DD\_M. A more consistent, stronger cold pool in DD\_M may be connected to the improved stratiform region (see Fig. 6).

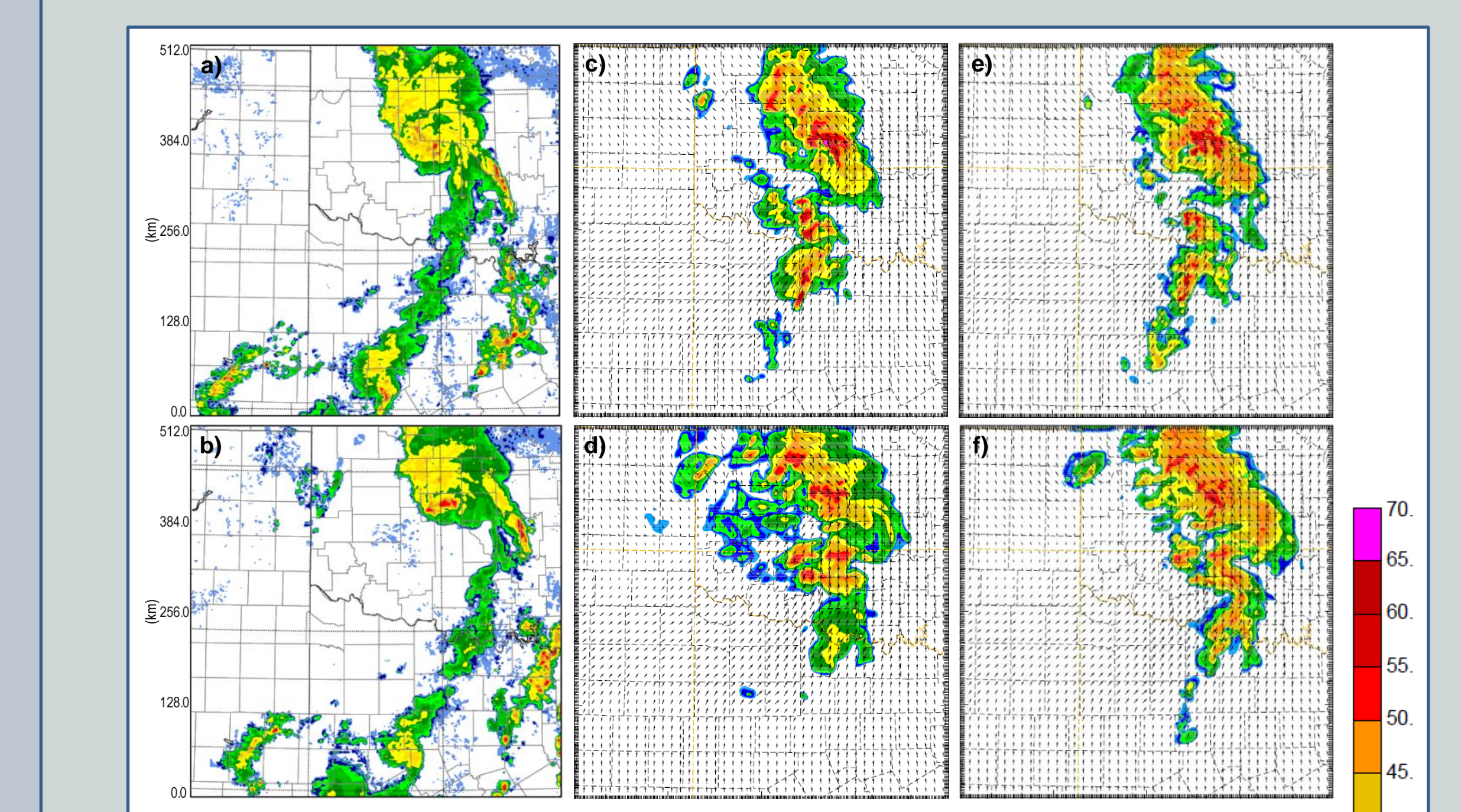


Fig. 9. Observed  $Z$  (dBZ) mosaics at (a) 0400 UTC and (b) 0500 UTC as well as (c) two hour (0400 UTC) and (d) three hour (0500 UTC) forecast  $Z$  for SS\_M, (e-f) SD\_M, (g-h) DD\_M, (i-j) DD\_MA, (k-l) DD\_R. The stratiform regions and convective line fit the observations better in DD\_M compared to DD\_MA and DD\_R. SD\_M begins to converge towards DD\_M between hours two and three.

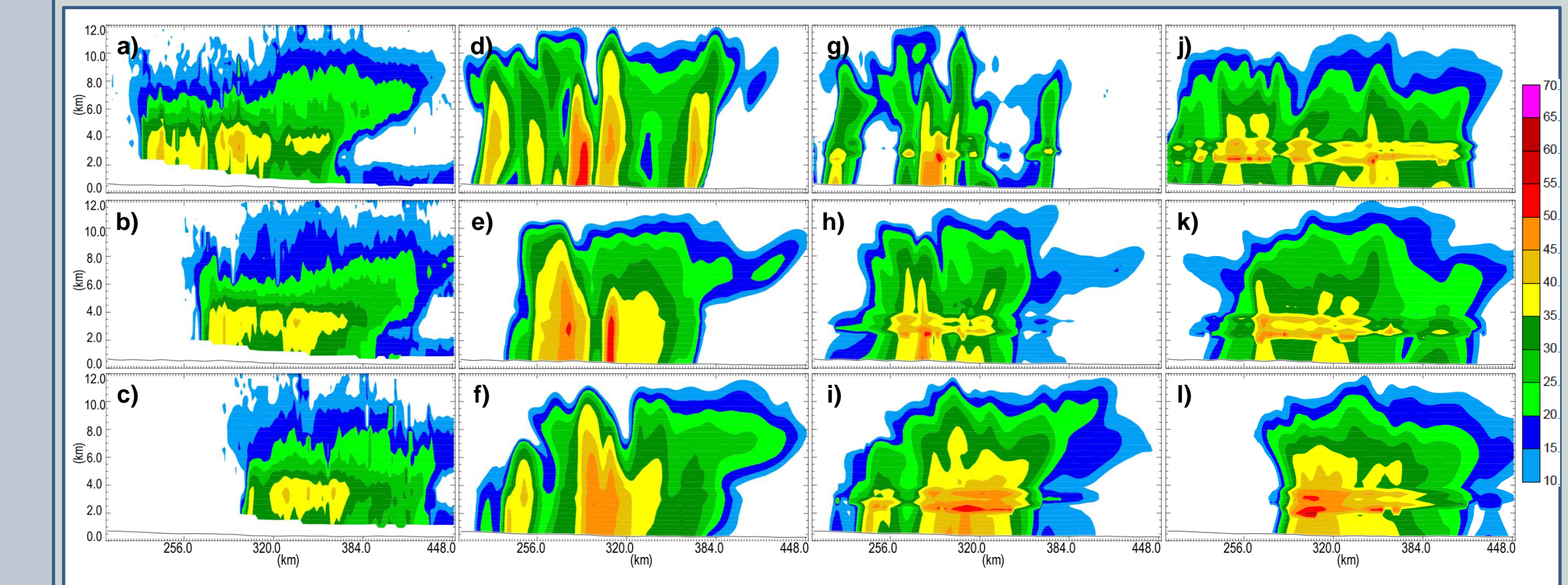


Fig. 10. Observed east-west vertical cross section of  $Z$  through the leading stratiform region from KTLX at (a) 0300 UTC, (b) 0400 UTC, and (c) 0500 UTC as well as east-west cross sections of  $Z$  for (d) one hour (0300 UTC), (e) two hour (0400 UTC), and (f) three hour (0500 UTC) forecasts from SS\_M, (g-i) SD\_M, and (j-l) DD\_M. While both SS\_M and SD\_M contain vertical, more convective development, the  $Z$  presentation is more consistent in east-west extent and stratiform in nature.

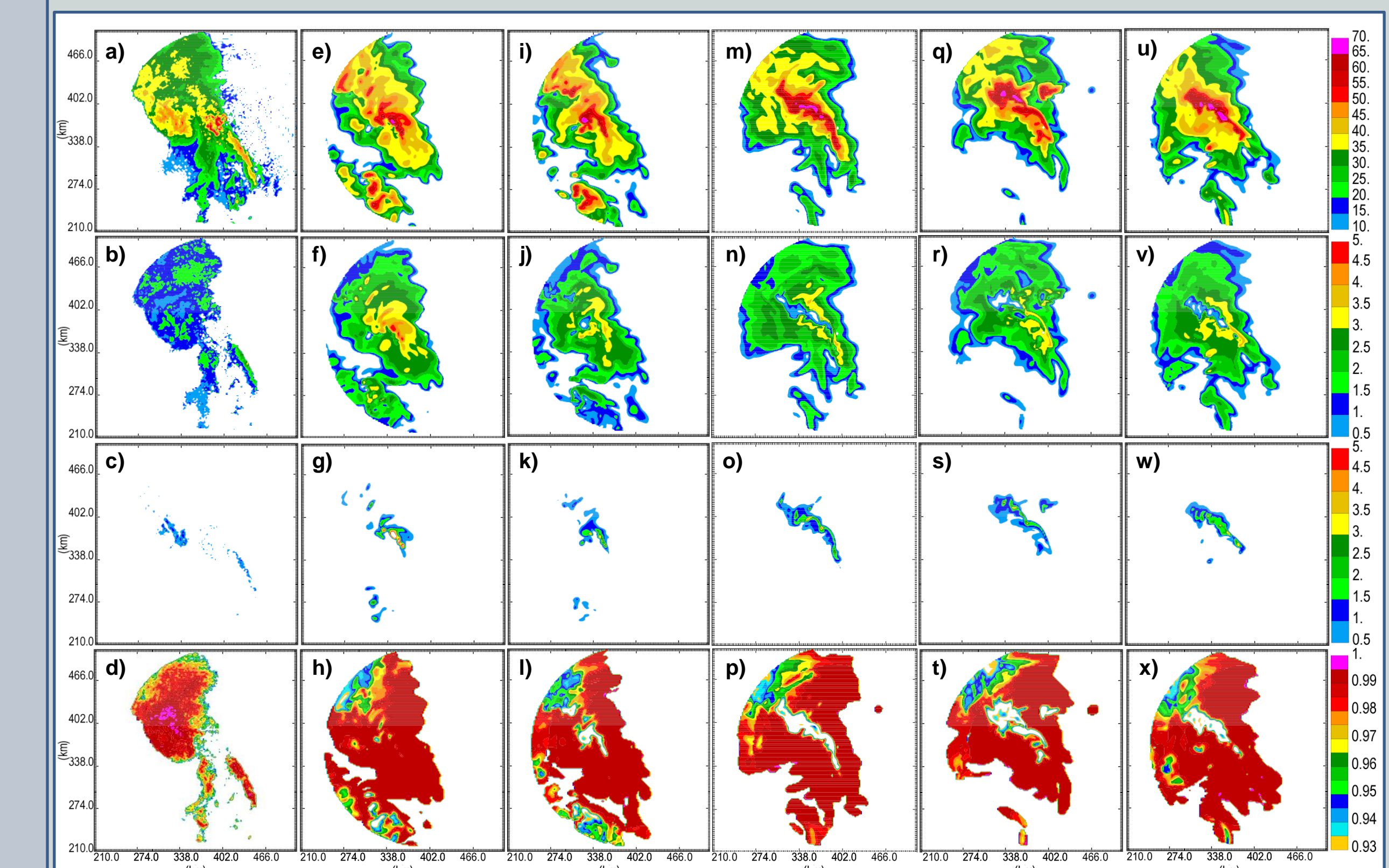


Fig. 11. Observed (a)  $Z$  (dBZ), (b)  $Z_{dr}$  (dB), (c)  $K_{dp}$  (dB km<sup>-1</sup>), and (d)  $\rho_{hv}$  from KOUN at 5' tilt as well as simulated variables for (e-h) SS\_M, (i-l) DD\_M, (m-p) DD\_MA, and (q-x) DD\_R from their respective two hour forecasts at 0400 UTC. Note that the simulated variables are as if they were observed from KOUN. Higher  $Z_{dr}$  values on the eastern edge of the leading convective line indicative of size sorting and more realistic  $K_{dp}$  values.

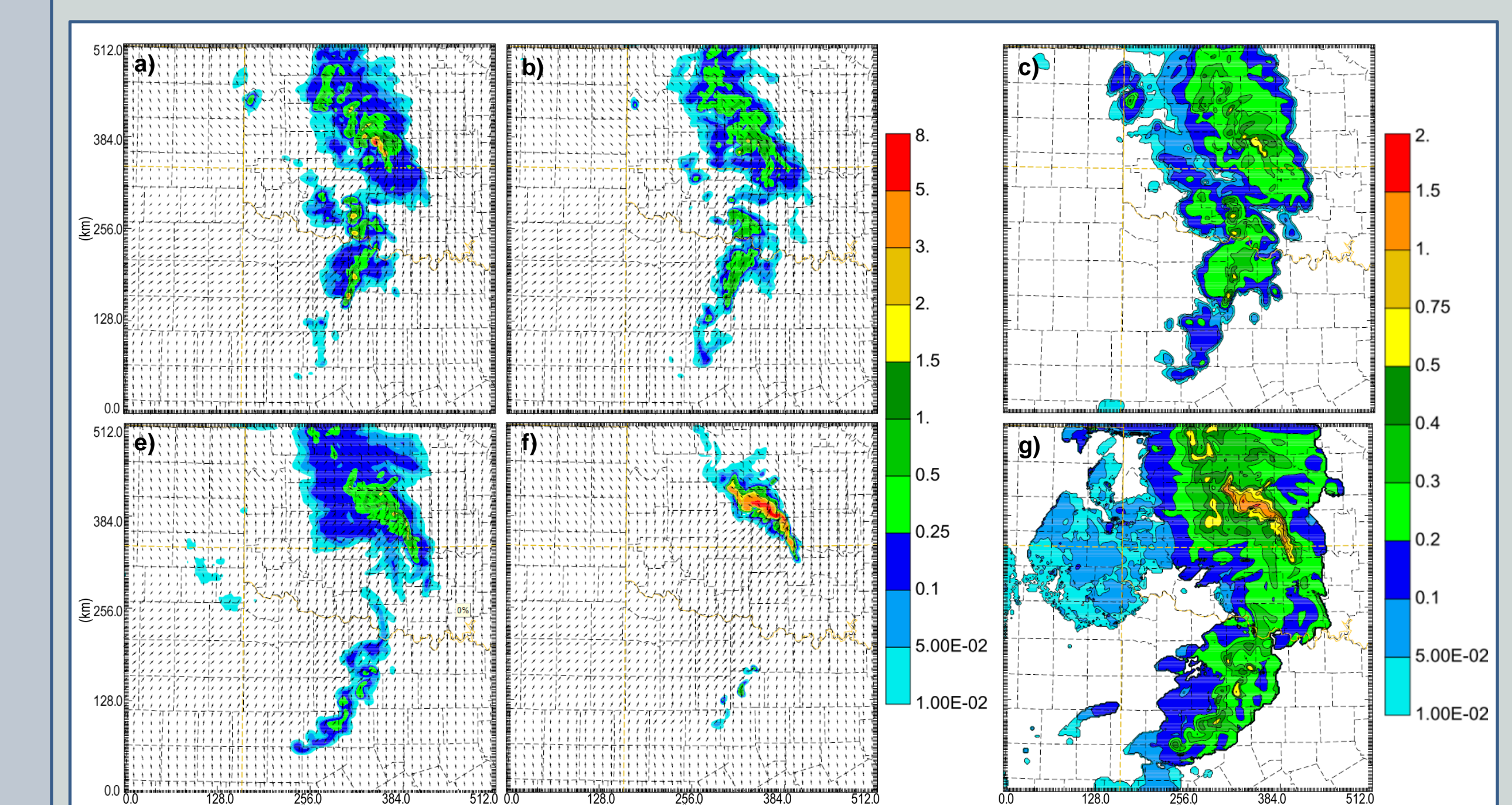


Fig. 12. Two hour forecast (0400 UTC) (a) rain and (b) hail mixing ratios ( $\text{g kg}^{-1}$ ) as well as (c) mass weighted median diameter (mm) for SS\_M as well as (d-f) DD\_M. DD\_M better represents expected differences in the amount of rain and median droplet diameter between the leading convective line and stratiform region.

## Conclusions

- Both SS\_M and SD\_M were poor in terms of structure and microphysical state and contained spurious convection. However, SD\_M improved near the end of the forecast period as the system adjusted to the DM scheme.
- Use of DM scheme during assimilation provided a better representation of the microphysical state of the system, specifically the size sorting of hydrometeors in the leading convective line and the size of raindrops in the stratiform regions.
- The DD\_M forecast showed significant improvement in the structure of the system, including the breadth and vertical composition of the leading stratiform region and extent of the trailing stratiform region and leading convective line.
- The DD\_M forecast also showed improvement in the size sorting of droplets in the leading convective line and the size of droplets in the stratiform regions, as in the final analysis.
- More significant improvement in DD\_M was hampered by excessive hail production. An experiment with graupel instead of hail resulted in excessive large rain and no structural improvement (not featured).
- DD\_MA analysis contained excessive hail and had a poorer  $Z$  fit to the observations in the stratiform region in the forecast.
- DD\_R had a poorer handle on the leading convective line and the extent of the stratiform region was greater than observed.

This work was supported by the NSF. The authors would like to thank the OU Supercomputing Center for Education and Research (OSCCER) and the National Institute for Computational Sciences for the use of their supercomputers.

\* Corresponding author address: Bryan J. Putnam, National Weather Center, Suite 5240, 120 David L. Boren Blvd, Norman, OK 73071; bryan.j.putnam-1@ou.edu